International Journal of Environmental Science and Technology
https://doi.org/10.1007/s13762-021-03705-4

ORIGINAL PAPER

Electrospun polyacrylonitrile nanofiber membranes for air filtration application

V. S. Naragund[1,2] · P. K. Panda[1,2]

Received: 14 February 2021 / Revised: 20 August 2021 / Accepted: 26 September 2021

Abstract

Polyacrylonitrile (PAN) nanofiber membranes of varied thicknesses (20–100 µm) were electrospun at a polymer concentration of 14% (w/v) in *N*,*N*-Dimethylformamide (DMF); characterized for porosity, pressure drop, air permeability and particle filtration efficiency (PFE). Densities of membranes are found very less (0.11 to 0.21 g/cm^3), with porosities in the range of 80–92%, higher porosity was for higher thickness. Membranes were used to measure air pressure drop, which was higher for thicker membranes due to the torturous path encountered by air. Air permeability of membranes decreased with increasing thickness for the same reason. The PFE was higher for thin samples due to less porosity and was lower for thicker samples due to higher porosities and cushion effect. The 20-µm-thick membranes achieved highest PFE of > 99.7% for clearing 0.3 µm particles. Above experiments suggested that PAN nanofiber membranes prepared in this study could be used for face mask in addition to non-woven fabrics.

Keywords Electrospinning · Polyacrylonitrile · Nanofiber membrane · Air filters · Pressure drop

Introduction

In today's world, air is contaminated by fine particulates, biological pathogens, as well as acidic vapors/gases. These contaminants are harmful to human body and can cause many diseases. For example, inhalation of particulate materials such as fine dust and pollens can trigger diseases such as asthma, blockage and reduction in lung capacity. Further, any carcinogens in engine exhaust, cigarette smoke, chemical vapors may cause chronic obstructive pulmonary disease (COPD) (Brunekreef and Holgate 2002). Therefore, air contaminations are bigger problems which throw challenges to scientists and engineers to develop/invent methods for their purification.

International Organization for Standardization (ISO/TC142 2016 Air filters for general ventilation—Part-1) has classified particulate matter (PM) into four categories depending on the aerodynamic size (x) range of the particle: (i) PM1: $0.3 \le x \le 1$ µm, (ii) PM2.5: $0.3 \le x \le 2.5$ µm (iii) PM10: $0.3 \le x \le 10$ µm. Particles with size range of 0.5 to 5 µm or smaller can deposit on lungs and, thus, can reduce the lung capacity eventually leading to lung failure. PM with less than 0.2 µm is even more dangerous as they can pass through respiratory system and eventually reaches in blood stream after penetrating through alveoli, resulting in artery vasoconstriction (Rundell et al. 2007). Air pollution in India is very high due to high population, manufacturing industries, poor road infrastructure, etc. A recent data from World Health Organization (WHO Ambient Air Quality Database Application 2016) have indicated that India and China are major contributors for PM2.5 & PM10 pollution (Fig. 1a). With world's top ten highly polluted cities present in India, the risk of air pollution is a greater concern (Fig. 1b). Therefore, cleaning of air to exclude PM, especially, fine particles from air is gaining significance.

Electrostatic precipitation (Mizuno 2000) technique is commonly used for cleaning of thermal power plant exhaust. Frequent servicing is required to remove dust from the electrodes used in this equipment. Membranes or mechanical

Editorial responsibility: M. F. Yassin.

✉ P. K. Panda
pkpanda@nal.res.in

[1] Materials Science Division, CSIR – National Aerospace Laboratories, Old Airport Road, Kodihalli, Bengaluru 560017, India

[2] Academy of Scientific and Innovative Research (AcSIR), Ghaziabad 201002, India

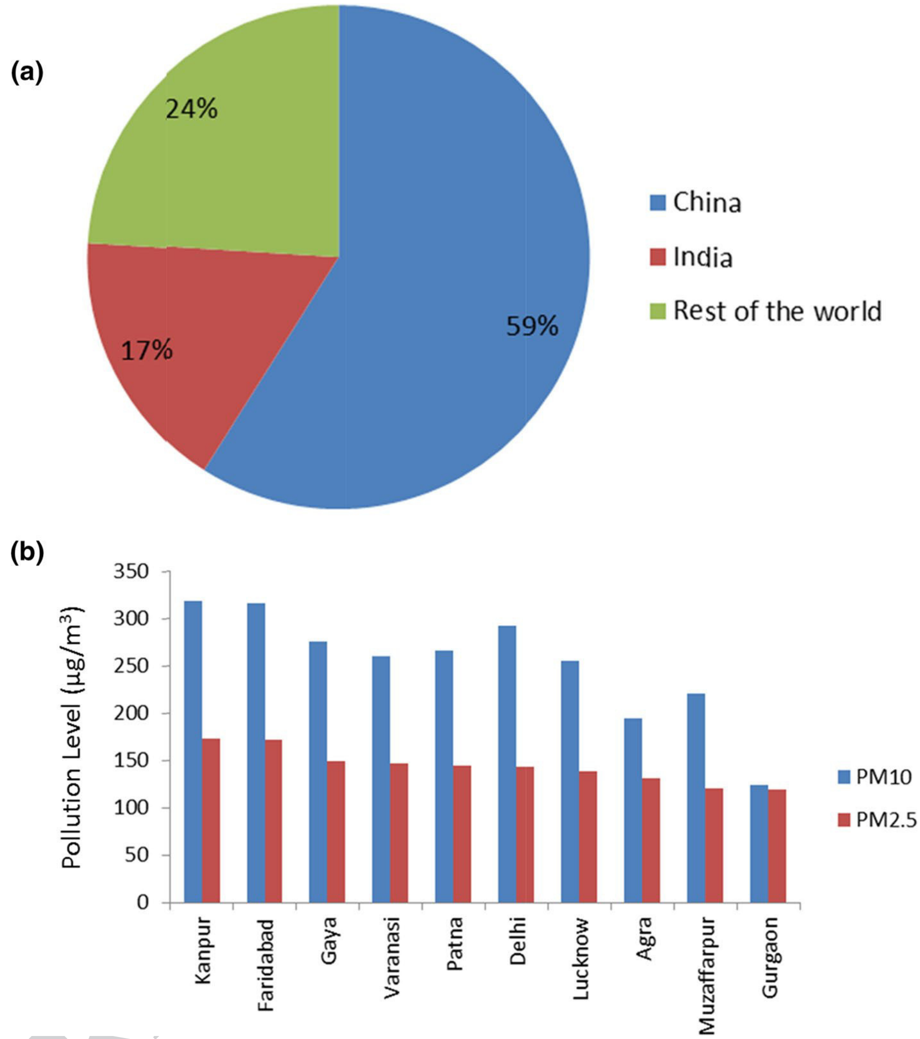

Fig. 1 **a** Contribution of particulate matter (PM2.5) air pollution by top 100 most polluted cities by country wise, **b** particulate matter concentration (PM2.5 & PM10) in top 10 cities around the world in year 2016 (Data source: WHO Ambient Air Quality Database Application [4])

filters have been used for air cleaning units in buildings, personal protection, engine intake, etc. The conventional membrane media commonly used are microglass fiber, cellulose paper or polyester bags. They have low initial filtration efficiency for particles of size less than 300 nm due to bigger fiber sizes, and blockage of their internal pores leading no reusability.

Nanofiber filter media offer several advantages due to small fiber size which are comparable to mean free path of air molecule. Nanofibers in flat sheet/membrane form are preferably prepared by electrospinning process (Barhoum et al. 2019; Panda and Sahoo 2013) which is simple and scalable method that utilizes high-voltage electric fields applied to polymer solutions. Electrospun nanofiber membrane filters are increasingly used in air filtration applications due to combination of well-desired properties such as: (i) lower pressure drops observed because air molecules slips around the nanofiber (Zhao et al. 2016) and nanofiber incorporated face mask had lower pressure than a N95 respirator providing similar filtration efficiency (Skaria and Smaldone 2014); (ii) higher filtration efficiency for small particles due to smaller inter-fiber pore size in nanofiber membranes w.r.t conventional media at similar pressure drop (Bortolassi et al. 2019a, b). In industry, Clarcor's UAS ProTura® filter with a nanofiber layer has demonstrated 50% longer life and achieved > 85% particle filtration efficiency (PFE) for submicron particles; (iii) possibility of reuse by knocking off dust layer formed on the surface of fine nanofibers using reverse air pulse (Wang et al. 2016).

The PFE of electrospun nanofiber membranes can be tuned by varying fiber morphology, diameter, transparency/thickness of membranes (Hau and Leung 2016; Jing et al. 2016; Zhang et al. 2016). Moreover, Leung et al. (2009) compared microfiber and nanofiber filters and found that nanofiber membrane has high filtration efficiency than microfiber. Bortolassi et al. prepared antimicrobial

Journal : Large 13762	Article No : 3705	Pages : 12	MS Code : 3705	Dispatch : 1-10-2021

nanofiber-based filters membranes which can achieve ~ 100% filtration efficiency (Bortolassi et al. 2019a, b). However, behavior of electrospun nanofiber membranes across wide range inlet pressures and flow rates for different thickness were not reported in the literature. Also, the inter-fiber distance seems to be an important parameter governing filtration property is missing or discussed in only few reports (Li and Gong 2015; Choi et al. 2018).

The hydrophilic nature of polyacrylonitrile (PAN) aids in moisture transfer from the human body (Dong et al. 2014; Valipouri et al. 2018) thus providing comfort. Therefore, in this work, PAN was used as a model polymer due to hydrophilicity and good fiber forming ability. Firstly, 10–14% w/v PAN in *N*,*N*-Dimethylformamide (DMF) solutions was carried out to study morphology of nanofibers. Then, 14% w/v PAN was studied in detail because it quickly gained thickness facilitating the study in wide thickness range (20 to 100 µm). The novelty of this work is analyzing the dependencies of air filtration properties such as pressure drop, air permeability, and filtration efficiency on porosity/thickness of the PAN membrane toward face mask application. Also, X-ray photoelectron microscopy (XPS) and sessile drop studies were carried out to investigate the surface wetting properties of the membrane. Finally, airborne particle filtration characteristics were also correlated to inter-fiber spacing. The present study was performed in Materials Science Division, CSIR-National Aerospace Laboratories, Bengaluru (India) during 2019–2020.

Experimental

Materials

PAN (Mw ~ 150,000 g/gmol; CAS number 25014-41-9) was purchased from M/s Sigma-Aldrich. N, N- Dimethyl formamide (DMF; 99.0%; CAS number 68-12-2) procured from M/s. SDFCL, India was used as solvent. Both chemicals were used without further purification.

Preparation of PAN solution and electrospinning of membranes

The PAN solution preparation was already described elsewhere (Naragund and Panda 2018). The method was adopted with slightly modification by using heat while stirring in this study. Briefly, measured amount of PAN, i.e., 1 g, 1.2 g and 1.4 g was added in 10 ml DMF to achieve 10, 12 and 14% (w/v) solutions, respectively, after stirring for about 6 h on a hot plate magnetic stirrer (IKA C-MAG HS4) set at about 60 °C. The solution was cooled to room temperature and loaded in 10 ml syringe with 24 gauge needle (0.55 mm needle). While the needle tip was connected to high-voltage power supply, rotating aluminum drum collector (diameter: 80 mm, 700 ± 60 rpm) attached on sliding table was connected to ground. The high voltage was increased till a stable polymer jet was visible. Fibers were collected on an aluminum foil warped on rotating drum. The time of electrospinning varied from 10, 20 and 40 min to prepare membranes of different thickness/coating levels. The uniformity of thickness in membranes was ensured by sliding motion (10 cm) of the collector table. The electrospinning conditions are provided in Table 1. It was observed that 14% solution was quickly able to form better membranes of wide thickness range; therefore, it was used in further experiments.

Characterization of nanofiber membranes

Morphology of nanofibers

The morphology and diameter of the electrospun w.r.t polymer concentrations is observed fibers on Carl Zeiss EVO 18 scanning electron microscope. Diameter distribution of the nanofibers is plotted by measuring diameters of about 25–30 fiber diameters on SEM images. Inter-fiber distance was also measured on SEM image of 10,000 × magnification.

Table 1 Solution preparation and electrospinning conditions for electrospinning

Chemical precursor	Preparation of solution	Electrospinning conditions
(i) Polyacrylonitrile (PAN) (Mw = 1,50,000) (ii) Dimethylformamide (DMF)	10–14% w/v PAN/DMF; 60 °C stir for 5–6 h	(i) Needle: 24 Gauge, 0.55 mm outer diameter (ii) Tip to collector distance (TCD): 10 cm (iii) DC Voltage: 18.5 kV (iv) Flow rate: 2.5 ml/h (V) Relative humidity: 65%

Journal : Large 13762 | Article No : 3705 | Pages : 12 | MS Code : 3705 | Dispatch : 1-10-2021

Physical properties of nanofiber membranes

Circular nanofiber samples ($\varphi = 47$ mm diameter) were punched out. Weight (w) and thickness (t) of the samples were measured on weighing balance and vernier caliper (± 0.01 mm), respectively. The apparent density (∂_n) of the nanofiber mats of different thickness is calculated by Eq. (1).

$$\text{Apparent density}(\partial_n) = \frac{w}{\pi \times \frac{\varphi^2}{4} \times t} \tag{1}$$

The apparent porosity (α) of mats is calculated by using Eq. (2)

$$\text{Apparent porosity}(\alpha) = \left(1 - \frac{\partial_n}{\text{Bulk density of PAN}}\right) \times 100\% \tag{2}$$

where bulk density of PAN as specified by manufacturer is 1.184 g/cm^3.

Specific area weight (W_a) of the nanofiber sample is calculated by using Eq. (3)

In order to remove moisture by wicking and cause comfort to wearer, membrane materials should be hydrophilic in nature. Therefore, contact angle of PAN nanofibers was measured by sessile drop method on a contact angle meter (Apex instruments, India) to determine surface wetting property of the PAN nanofiber membrane. About 8 µl of DI water was dropped on the PAN nanofiber surface, and contact angle was measured by recording images on the system.

Air permeability test

Air permeability of nanofiber membranes was measured on a custom built setup as shown schematically in Fig. 2. The setup holds the membrane securely, exposing ~ 19.6 cm^2 (diameter ~ 5 cm) of membrane surface area for perpendicular air flow while holding the membrane securely. Three samples were tested for each thickness. For testing, the inlet air flow rate through the membrane is slowly adjusted and flow rate corresponding to certain pre-defined pressure drop is noted as per ISO standard (ISO/TC 38 1995). The air permeability of nanofiber membrane is calculated by Eq. (4).

$$\text{Air permeability}\left(\frac{L}{m^2 s}\right)\text{at a pressure drop} = \frac{\text{Air flow rate}\left(\frac{L}{s}\right)}{\text{Effective area of sample}\left(m^2\right)} \tag{4}$$

$$\text{Specific area weight }(W_a) = \frac{4W}{\pi\varphi^2} \tag{3}$$

Fourier transform infrared spectroscopy (FTIR)

The PAN nanofiber membrane was cut into small pieces and mixed with KBr powder using mortar and pestle to prepare sample in pellet form. The ATR-FTIR spectra of pellet sample were recorded 16 times with a resolution of 4 cm^{-1} in the range of 4000 to 400 cm^{-1} on PerkinElmer Frontier machine.

X-ray photoelectron spectroscopy analysis

The surface chemical compositions of PAN nanofibers were analyzed by XPS (SPECS GmbH) with non-monochromatic Al Kα radiation (1486.6 eV) operated at 150 W (12 kV, 12.5 mA).

Contact angle measurements

Exhaled human breath contains moisture with relative humidity ranging from 40 to 90% (Mansour et al. 2020).

where effective area of sample is ~ 19.6 cm^2 in the study.

Pressure drop measurements

The pressure drop across thickness of nanofiber membranes was also measured on above setup. The pressure drop experiments were carried out to study the behavior of membranes at varied air pressures, air flow rates, and for different membrane thicknesses. Due to compressor limitation, pressures up to 6 kg/cm^2 were tested. A differential pressure gauge (diaphragm type, ± 25 Pa) connected between inlet and outlet manifold is used to indicate the pressure difference/drop across the membrane. The air flow rates in the range of 5 to 50 l/min were used, because human breathing rate in moderate work falls within this range (Zuurbier et al. 2009).

Measurement of PFE

In this experiment, air from compressor containing airborne particles was passed through the setup (Fig. 2) at 5 kg/cm^2 and 50 l/min. A laser particle counter system (CLJ-BII, Honri Airclean Tech., China) was used to measure the upstream (C_u) and downstream airborne particle count (C_d),

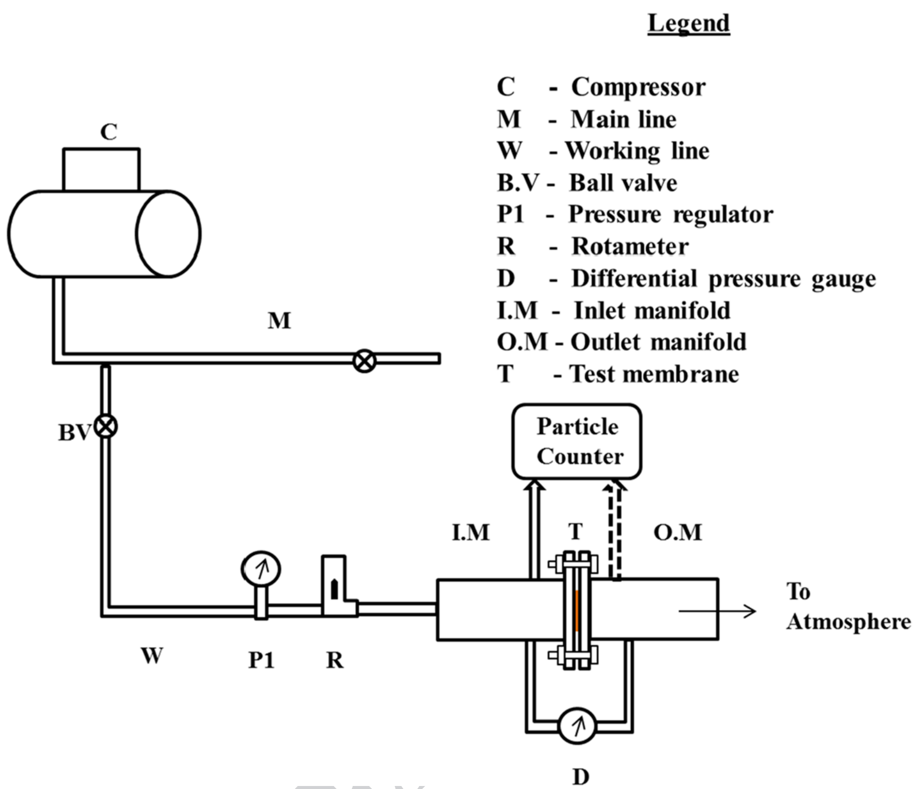

Fig. 2 Schematic of experimental setup used for measuring filtration properties of electrospun nanofiber membrane

i.e., before and after the nanofiber membranes. In particle counting, air was drawn automatically into the system at fixed rate of 2.8 L/min and sampled over a time period of 60 s to make particle count at five different particle sizes (0.3, 0.5, 1.0, 3.0, 5.0 µm). Filtration efficiency of nanofiber filter membrane is calculated using Eq. 5.

$$\mathrm{PFE}(\eta) = 1 - \frac{C_d}{C_u} \quad (5)$$

Results and discussion

Morphology of nanofibers

The morphology and diameter distribution of the electrospun PAN nanofibers w.r.t polymer concentrations are presented in Fig. 3. It is observed that diameters of fibers were in the range of 80 to 600 nm, and the average diameter increased with the increase in polymer concentration (Naragund and Panda 2018). In this work, fiber diameters were higher than earlier reported work (Naragund and Panda 2018) because of evaporative loss of solvent while stirring at higher temperature causing increase in viscosity of solution.

Relation between porosity and electrospinning duration

The thickness and specific area weights of nanofiber membranes prepared at different electrospinning time durations are provided in Table 2. The thickness, as well as specific area weight, of the membranes increased with electrospinning duration. The plot of membrane thickness and electrospinning duration vs. apparent porosity is shown in Fig. 4. Three samples were tested for each thickness. It is observed that apparent porosity of the membrane increased with increasing thickness/duration of the membranes. Xiang et al. (2011) also reported similar trend. This is due to charge accumulation on fibers created inter-fiber repulsions leading to higher porosity creating a *cushion effect* in higher thickness membranes.

FTIR spectroscopy

The FTIR spectrum of PAN nanofibers is presented in Fig. 5. The characteristic vibrations of polyacrylonitrile are observed at 2937 cm^{-1} due to stretching vibrations of methylene (CH_2) and 2243 cm^{-1} stretching of C≡N (nitrile) groups (Aykut et al. 2013). The peak at 1452 cm^{-1} is due to

Journal : Large 13762 | Article No : 3705 | Pages : 12 | MS Code : 3705 | Dispatch : 1-10-2021

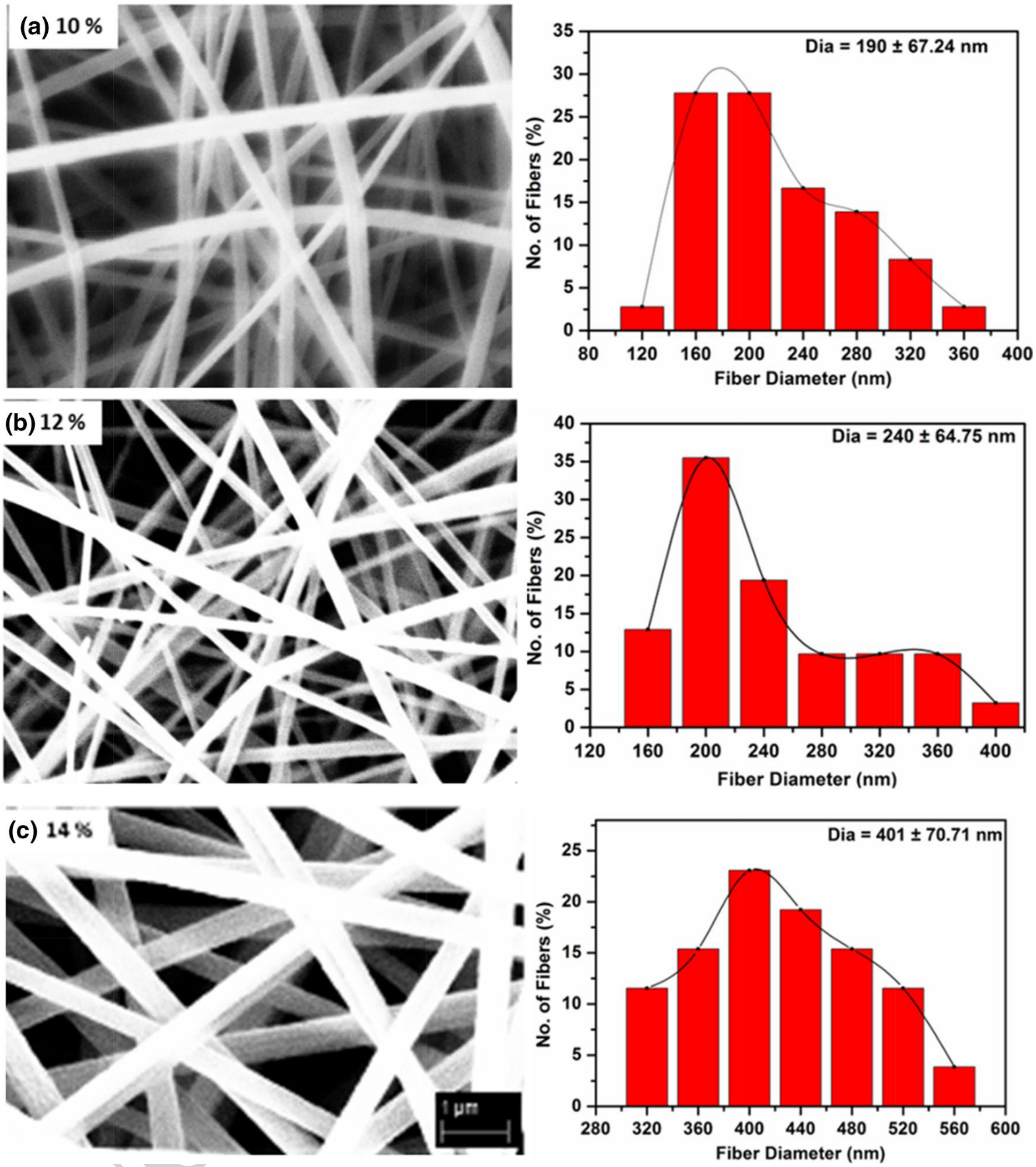

Fig. 3 SEM micrograph (10,000 ×) and corresponding diameter distribution of PAN nanofibers electrospun at different PAN/DMF concentrations

Table 2 Thickness and specific area weight of PAN nanofiber membranes electrospun for different lengths of time

Time of electrospinning (min)	Thickness (mm)	Density (g/cc)	Specific area weight (g/m^2)
10	0.02 ± 0.01	0.214 ± 0.035	4.613 ± 0.557
20	0.04 ± 0.01	0.164 ± 0.017	6.440 ± 1.013
40	0.10 ± 0.01	0.114 ± 0.017	12.110 ± 2.079

the bending vibration of CH_2 group. The peak at 1690 cm^{-1} is assigned to the stretching of C=O of residual DMF. The observed peaks matched closely with literature reported (Yu et al. 2012; Aykut et al. 2013).

XPS analysis

The surface compositions of the nanofibers were studied further using XPS analysis. The survey XPS spectrum and

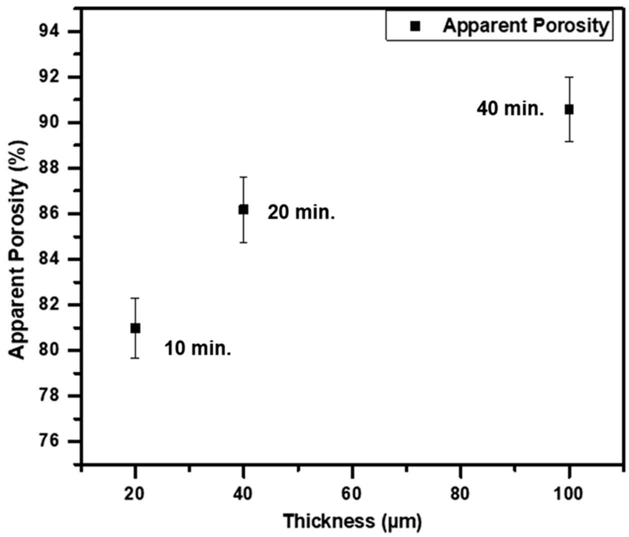

Fig. 4 Thickness vs. porosity of PAN nanofiber membranes prepared by electrospinning for different lengths of time

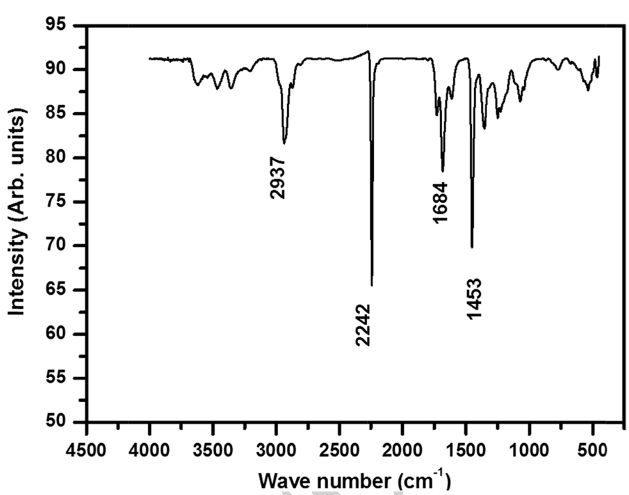

Fig. 5 ATR-FTIR spectra of PAN nanofibers

N 1s spectra of PAN nanofibers are shown in Fig. 6a, b. The survey spectrum exhibits three intense peaks at 284.9, 398.5 and 532.6 eV corresponding to C 1s, N 1s, and O 1s core levels respectively. The oxygen peak at 532 eV is due to water molecules adsorbed on fiber surface (Tas et al. 2016; Goodacre et al. 2020). The high-resolution XPS spectra N 1s spectra shown in Fig. 6b have a peak centered at about 398.5 eV due to the presence of C≡N groups in PAN (Takahagi et al. 1986; Wang et al. 2013).

Contact angle measurement

The water contact angle of the PAN nanofiber membranes is shown in Fig. 7. The average contact angle of nanofiber membranes was ~ 81°, < 90°which indicates that PAN membranes are slightly hydrophilic nature. This hydrophilic nature is attributed to moisture adsorbed on PAN nanofibers (Alarifi et al. 2015). AQ2

Filtration properties of nanofiber membranes

Air permeability

The air permeability of membranes of different thickness was measured at three pressure drops: 100, 150 and 200 Pa and presented in Table 3. It was observed that at constant membrane thickness, the air permeability increased with increasing pressure drops. For membranes of variable thickness, the air permeability was higher for lower thickness due to less torturous path encountered during the air passage. The measured air permeability for the nanofiber membranes was the range reported in the literature. (Kucukali-Ozturk et al. 2017; Ruan et al. 2020).

Pressure drop across nanofiber membrane

The pressure drop across nanofiber membranes as function of air flow rates for different thicknesses at various inlet

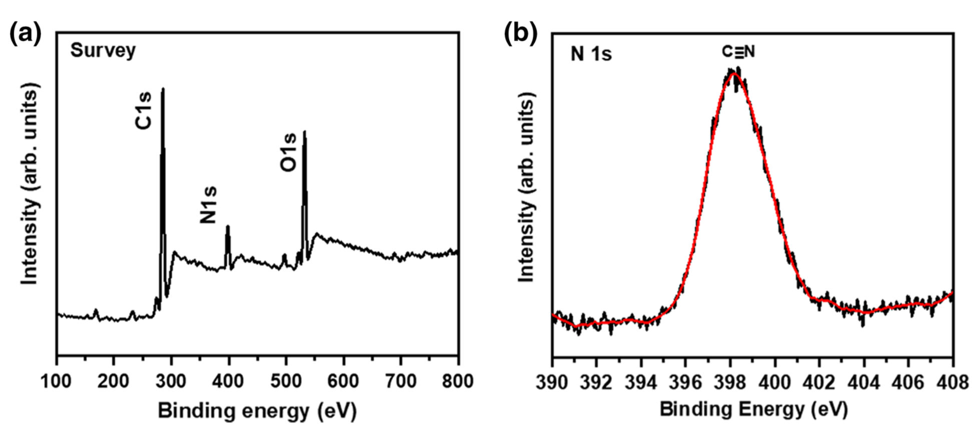

Fig. 6 **a** XPS survey and **b** high-resolution XPS spectra of N 1s of PAN nanofiber

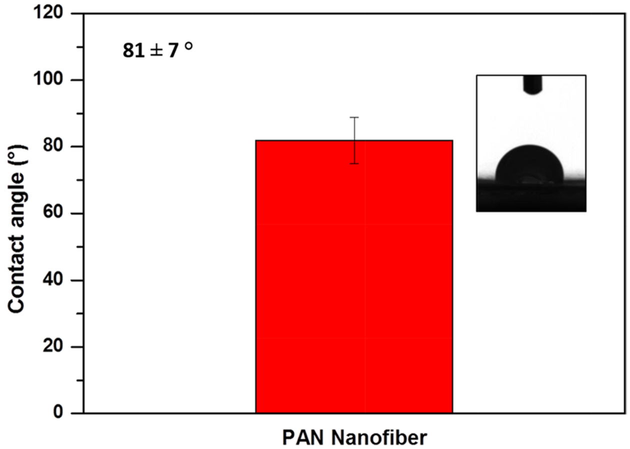

Fig. 7 Water contact angle of electrospun PAN nanofiber membrane

Table 3 Pressure drops and corresponding air permeability for membranes at different thickness

Thickness (mm)	Pressure drop (Pa)	Air permeability (l/m^2 s or mm/s)
0.02 ± 0.01	100 ± 25	218.2 ± 14.4
	150 ± 25	257.9 ± 10.6
	200 ± 25	289.1 ± 13.8
0.04 ± 0.01	100 ± 25	60.9 ± 5.3
	150 ± 25	80.7 ± 3.4
	200 ± 25	102.0 ± 6.9
0.100 ± 0.01	100 ± 25	45.3 ± 4.0
	150 ± 25	59.5 ± 6.94
	200 ± 25	70.8 ± 4.0

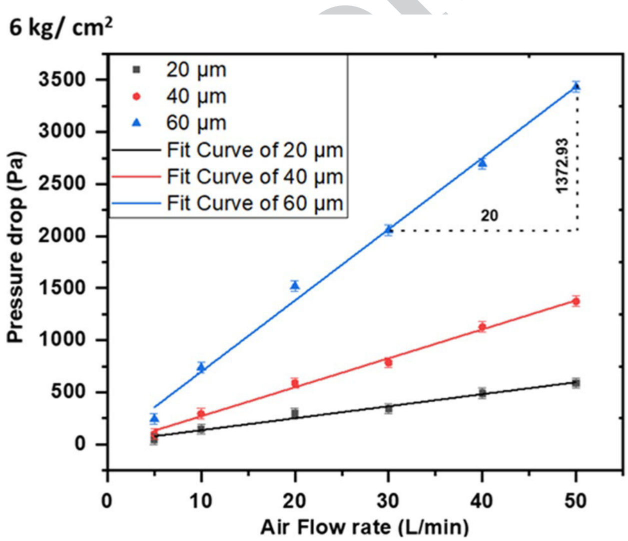

Fig. 8 Pressure drop vs. air flow rates for nanofiber membranes of different thicknesses at 6 kg/cm^2 inlet pressure

pressures (1–6 kg/cm^2) was measured. Since, pressure drop for different inlet pressures was observed to be almost the same range, a typical behavior of membranes at 6 kg/cm^2 is presented in Fig. 8. It was seen that pressure drop increased linearly with air flow rates. Similar results were obtained when face velocity of air was increased (Bortolassi et al. 2019a, b). The pressure drop was higher (250 to 3500 Pa) for higher thickness (100 μm) membranes, because larger tortuous path encountered to the air flowing inside the membrane. Linear fitting of the data showed a higher slope of 68.45 for 100 μm membrane vs. slope of 11.66 for thinner membrane of 20 μm, indicating quicker rise in the pressure drop in the case of thicker membrane.

Filter mask materials with lower pressure drops are desirable as they support easier breathing with minimum efforts. The benchmark for the pressure drop according to the filtration standards for face mask, the British standard EN 14683 (Medical face masks—Requirements and test methods, 2019) for medical face mask is < 40 Pa/cm^2 across the membrane at air flow rate of 8 l/min. Therefore, the pressure drop (Pa/cm^2) across nanofiber membranes of different thickness is measured at flow rate of ~ 10 l/min and presented in Table 4. From this table, it can be seen that membranes of thickness 20 and 40 μm had pressure drops of 7.5 and 15.01 Pa/cm^2, respectively, which are < 40 Pa/cm^2, showing acceptable pressure drop.

PFE test

To measure PFE of a nanofiber membrane, first upstream particles were counted for three times, and then, a membrane of a particular thickness was fixed and downstream particles were counted. The experiments were repeated for three test membranes of other thickness. Figure 9 shows the airborne particle filtration efficiency at different particle sizes for electrospun nanofiber membranes. From the figure, it is seen that 20 μm membrane was an optimal thickness that filtered particles of all sizes effectively. Filtration efficiency was high at lower thickness of the membrane. The filtration efficiency decreased with increasing thickness. This is because of higher porosity and cushion effect in higher thickness membranes as discussed previously. At lower thickness, fibers were collected near to aluminum foil in dense manner due to quick charge dissipation, thus resulting in low porosity of membranes. This leads to higher filtration efficiency for thinner samples. The efficiency of membranes in reducing airborne dust of ~ 0.3 μm for all membranes was > 95%, as seen from the red vertical line A, drawn considering PFE of the three membranes at about 0.3 μm in Fig. 8 and Table 4.

Table 4 Pressure drop and filtration efficiency for membranes of different thicknesses

Average thickness (mm)	Particle filtration efficiency (%)[b]	Pressure drop per unit area (Pa/cm^2)[a]	Benchmark pressure drop
0.02 ± 0.01	99.71 ± 0.05	7.50 ± 2.08	< 40 Pa/cm^2 across the membrane at air flow rate of 8L/min. (British standard EN 14683)
0.04 ± 0.01	99.14 ± 0.22	15.01 ± 2.08	
0.100 ± 0.01	95.66 ± 1.32	42.52 ± 2.08	

[a]Measured at 10 l/min flow

[b]0.3 μm particles from compressor air

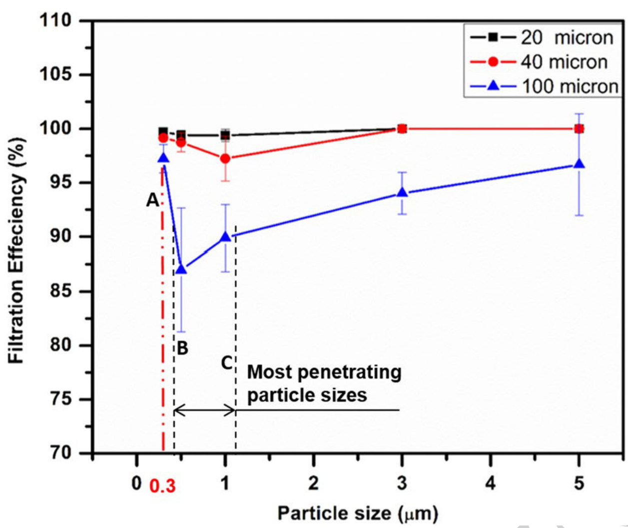

Fig. 9 Particle filtration efficiency for nanofiber membranes of different thicknesses at various particle sizes

Filtration model for electrospun nanofibers

The filtration model for electrospun nanofiber membranes is illustrated in Fig. 10. For fine particles, two mechanisms simultaneously drive filtration: (i) electrostatic attraction between small particles which are generally charged and electrospun fibers which carry charges inherently due to manufacturing process; (ii) loss of kinetic energy during zigzag path followed by fine particles between randomly oriented fibers and finally get trapped on the rough surface of nanofibers created due to evaporation of the solvent (Fig. 10a). For particles bigger than interstitial pore sizes, the particles get arrested/ trapped as shown in (Fig. 10b).

In a previous report, Li and Gong (2015) stated that lower inter-fiber spacing of nanofibers is a reason for higher filtration efficiency of nanofibers over microfibers. However, they did not measure inter-fiber spacing. So, in this work, inter-fiber spacing is measured and its distribution is presented in

Fig. 10 Particle filtration model of electrospun nanofibers

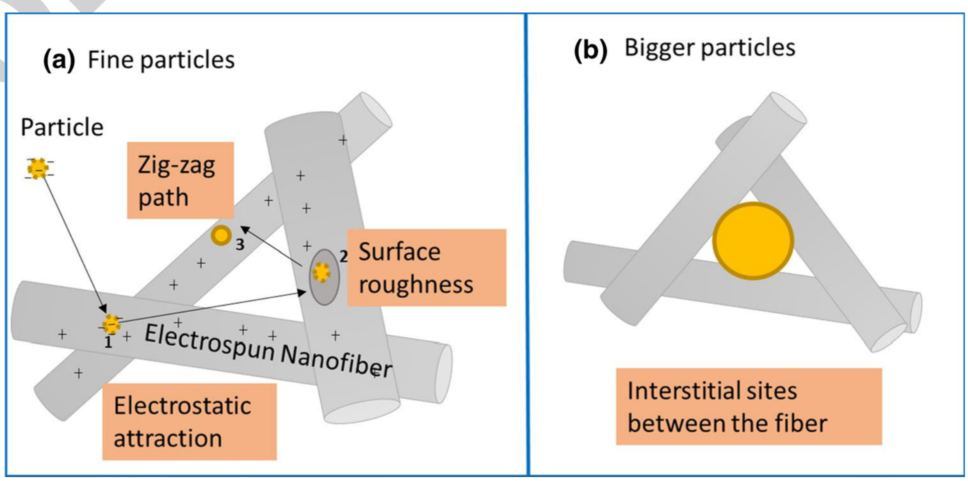

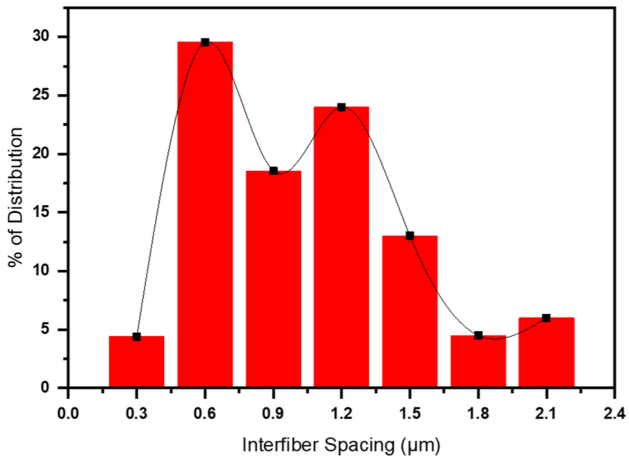

Fig. 11 Inter-fiber spacing histogram of 14% PAN nanofiber membrane

Fig. 11. It was found that higher peaks/distribution on histogram corresponds well with the most penetrating particle sizes, i.e., between 0.5 and 1.2 µm, which is represented by the vertical lines A and B drawn in Fig. 9.

Table 5 presents filtration properties of some commercially available nanofiber membrane mask, membranes reported in the literature and membranes tested in this study. It is seen by comparison that the membranes prepared in this study showed filtration efficiency nearly equivalent to those available in reported in the literature and commercial markets. Therefore, the membranes prepared in this work can also be used as face mask materials in addition to the already available nanofiber mask materials.

Conclusion

PAN nanofibers were electrospun using 10–14% PAN/DMF solutions, and 14% PAN nanofiber membranes of various thickness/porosities were prepared. The membranes were used for air filtration studies. Lower pressure drop (50–500 Pa) was observed across thinner membranes (~20 µm), and the pressure drop increased with the thickness and air flow rates. Air permeability and filtration efficiency increased with decreasing thickness. Higher filtration efficiency was observed for 20 µm thin membrane. The interfiber distance matched with most penetrating particle sizes found from the filtration experiments. The above experiments suggest that 20-µm-thick electrospun PAN nanofiber membranes could be suitable for air filtration applications such as face mask.

Table 5 Comparison of commercial, as well as nanofiber membranes, reported in the literature and membrane studied in the present work

Sl no.	Membrane	Filtration efficiency
1	M/s FNM RespiNano mask (FFP3, EN 149) Iran	> 99%[a]
2	M/s NASK nanofiber smart mask, Hong Kong, China	> 99%[a]
3	M/s Respilon 57 Antismog Scarf (R-Shield), Czech Republic	99% diesel fumes[a]
4	M/s Respilon® Filtration half mask (FFP2, EN 149:2009), Czech Republic	≥ 98.78%[a], 0.26 µm NaCl particle
5	Li and Gong (2015)	~ 99.4%
6	Bortolassi et al. (2019a, b)	~ 100%
7	Ruan et al (2020)	~ 99.99%
8	The present work	> 99.71% of 0.3 µm dust particles for nanofiber membrane of 20 µm thickness

[a]Values obtained from respective company brochures

Acknowledgements The authors thank Mrs Kalavati, and Mrs Latha S for technical assistance with SEM and XPS instruments, respectively. We thank Basuraj and Srinivasa from MSD workshop for their help in fabrication of filtration test setup. Thanks to Mr Harish K. and Mr Sureshkumar V. for assisting in filtration experiments. We also thank Mr M. Sagayaraj from M/s Trijama filters, Bengaluru for providing their help with particle counter used in this work. Mr. Veereshgouda S.N thanks CSIR, New Delhi for awarding SRF fellowship [31/003(0052)/2019-EMR-I].

Declarations

Conflict of interest The authors declare that they have no conflict of interest. The authors have no relevant financial or non-financial interests to disclose.

Ethical approval This article does not contain any studies with human participants performed by any of the authors.

References

Alarifi IM, Alharbi A, Khan WS, Swindle A, Asmatulu R (2015) Thermal, electrical and surface hydrophobic properties of electrospun polyacrylonitrile nanofibers for structural health monitoring. Materials 8(10):7017–7031

Aykut Y, Pourdeyhimi B, Khan SA (2013) Effects of surfactants on the microstructures of electrospun polyacrylonitrile nanofibers and their carbonized analogs. J Appl Polym Sci 130(5):3726–3735

Barhoum A, Pal K, Rahier H et al (2019) Nanofibers as new-generation materials: from spinning and nano-spinning fabrication techniques to emerging applications. Appl Mater Today 17:1–35. https://doi.org/10.1016/j.apmt.2019.06.015

Bortolassi AC, Guerra VG, Aguiar ML et al (2019a) Composites based on nanoparticle and pan electrospun nanofiber membranes for air filtration and bacterial removal. Nanomaterials 9(12):1740

Bortolassi C, Nagarajan S, de Araújo LB et al (2019b) Efficient nanoparticles removal and bactericidal action of electrospun nanofibers membranes for air filtration. Mater Sci Eng C 102:718–729

Brunekreef B, Holgate ST (2002) Air pollution and health. Lancet 360(9341):1233–1242

BS (2019) EN 14683 Medical face masks—requirements and test methods. BSI, London. https://shop.bsigroup.com/ProductDetail?pid=000000000030401487

Choi DY, An EJ, Jung SH, Song DK, Oh YS, Lee HW, Lee HM (2018) Al-coated conductive fiber filters for high-efficiency electrostatic filtration: effects of electrical and fiber structural properties. Sci Rep 8(1):5747

Dong Y, Kong J, Phua SL, Zhao C, Thomas NL, Lu X (2014) Tailoring surface hydrophilicity of porous electrospun nanofibers to enhance capillary and push–pull effects for moisture wicking. ACS Appl Mater Interfaces 6(16):14087–14095

Goodacre D, Blum M, Buechner C et al (2020) Water adsorption on vanadium oxide thin films in ambient relative humidity. J Chem Phys DOI 10(1063/1):5138959

Hau CWY, Leung WWF (2016) Experimental investigation of backpulse and backblow cleaning of nanofiber filter loaded with nanoaerosols. Sep Purif Technol 163:30–38

ISO (1995) Determination of the permeability of fabrics to air. ISO, Geneva

ISO (2016) Air filters for general ventilation—part-1: technical specifications, requirements and classification system based upon particulate matter efficiency (ePM). ISO, Geneva. https://www.iso.org/obp/ui/#iso:std:iso:16890:-1:ed-1:v1:en

Jing L, Shim K, Toe CY, Fang T, Zhao C, Amal R, Sun KN, Kim JH, Ng YH (2016) Electrospun polyacrylonitrile–ionic liquid nanofibers for superior PM 2.5 capture capacity. ACS Appl Mater Interfaces 8(11):7030–7036

Kucukali-Ozturk M, Ozden-Yenigun E, Nergis B, Candan C (2017) Nanofiber-enhanced lightweight composite textiles for acoustic applications. J Ind Text 46:1498–1510

Leung WWF, Hung CH, Yuen PT (2009) Experimental investigation on continuous filtration of sub-micron aerosol by filter composed of dual-layers including a nanofiber layer. Aerosol Sci Technol 43(12):1174–1183

Li X, Gong Y (2015) Design of polymeric nanofiber gauze mask to prevent inhaling PM2. 5 particles from haze pollution. J Chem 2015:460392

Mansour E, Vishinkin R, Rihet S, Saliba W, Fish F, Sarfati P, Haick H (2020) Measurement of temperature and relative humidity in exhaled breath. Sens Actuators B Chem 304:127371

Mizuno A (2000) Electrostatic precipitation. IEEE Trans Dielectr Electr Insul 7(5):615–624

Naragund VS, Panda PK (2018) Electrospinning of polyacrylonitrile nanofiber membrane for bacteria removal. J Mater Sci Appl 4(5):68–74

Panda PK, Sahoo B (2013) Synthesis and applications of electrospun nanofibers. In: Naveen N, Shishir S, Govil JN (eds) Nanotechnology vol. 1: fundamentals and applications, 1st edn. Studium Press, Texas, pp 399–416

Ruan D, Qin L, Chen R et al (2020) Transparent PAN:TiO2 and PAN-co-PMA:TiO2 nanofiber composite membranes with high efficiency in particulate matter pollutants filtration. Nanoscale Res Lett 15:7

Rundell KW, Hoffman JR, Caviston R, Bulbulian R, Hollenbach AM (2007) Inhalation of ultrafine and fine particulate matter disrupts systemic vascular function. Inhal Toxicol 19(2):133–140

Skaria SD, Smaldone GC (2014) Respiratory source control using surgical masks with nanofiber media. Ann Occup Hyg 58(6):771–781

Takahagi T, Shimada I, Fukuhara M et al (1986) XPS studies on the chemical structure of the stabilized polyacrylonitrile fiber in the carbon fiber production process. J Polym Sci Part A Polym Chem 24:3101–3107

Tas S, Kaynan O, Ozden-Yenigun E, Nijmeijer K (2016) Polyacrylonitrile (PAN)/crown ether composite nanofibers for the selective adsorption of cations. RSC Adv 6:3608–3616

Valipouri A, Farzin Z, Hosseini RS (2018) Investigating moisture management property of a bi-layer fabric through nanofiber-coated PET as a novel sewing thread: vertical wicking test. J Textile Polym 6(1):23–30

Wang J, Pan K, Giannelis EP, Cao B (2013) Polyacrylonitrile/polyaniline core/shell nanofiber mat for removal of hexavalent chromium from aqueous solution: mechanism and applications. RSC Adv 3:8978–8987

Wang C, Wu S, Jian M, Xie J, Xu L, Yang X, Zheng Q, Zhang Y (2016) Silk nanofibers as high efficient and lightweight air filter. Nano Res 9(9):2590–2597

Journal : Large 13762 | Article No : 3705 | Pages : 12 | MS Code : 3705 | Dispatch : 1-10-2021

WHO Ambient Air Quality Database Application (2016) World Heal Organ [accessed on 2020 Jun 10]. https://whoairquality.shinyapps.io/AmbientAirQualityDatabase/

Xiang HF, Tan SX, Yu XL, Long YH, Zhang XL, Zhao N, Xu J (2011) Sound absorption behavior of electrospun polyacrylonitrile nanofibrous membranes. Chin J Polym Sci 29(6):650–657

Yu DG, Chatterton NP, Yang JH, Wang X, Liao YZ (2012) Coaxial electrospinning with Triton X-100 solutions as sheath fluids for preparing PAN nanofibers. Macromol Mater Eng 297(5):395–401

Zhang R, Liu C, Hsu PC, Zhang C, Liu N, Zhang J, Lee HR, Lu Y, Qiu Y, Chu S, Cui Y (2016) Nanofiber air filters with high-temperature stability for efficient PM2.5 removal from the pollution sources. Nano Lett 16(6):3642–3649

Zhao X, Wang S, Yin X, Yu J, Ding B (2016) Slip-effect functional air filter for efficient purification of PM2.5. Sci Rep 6(1):35472

Zuurbier M, Hoek G, Van den Hazel P, Brunekreef B (2009) Minute ventilation of cyclists, car and bus passengers: an experimental study. Environ Health 8:48